

## Calcium Is a Cofactor of Polymerization but Inhibits Pyrophosphorolysis by the *Sulfolobus solfataricus* DNA Polymerase Dpo4<sup>†</sup>

Adriana Irimia, Hong Zang, Lioudmila V. Loukachevitch, Robert L. Eoff, F. Peter Guengerich, and Martin Egli\*

Department of Biochemistry and Center in Molecular Toxicology, Vanderbilt University, School of Medicine, Nashville, Tennessee 37232

Received December 9, 2005; Revised Manuscript Received April 3, 2006

**ABSTRACT:** Y-Family DNA polymerase IV (Dpo4) from *Sulfolobus solfataricus* serves as a model system for eukaryotic translesion polymerases, and three-dimensional structures of its complexes with native and adducted DNA have been analyzed in considerable detail. Dpo4 lacks a proofreading exonuclease activity common in replicative polymerases but uses pyrophosphorolysis to reduce the likelihood of incorporation of an incorrect base. Mg<sup>2+</sup> is a cofactor for both the polymerase and pyrophosphorolysis activities. Despite the fact that all crystal structures of Dpo4 have been obtained in the presence of Ca<sup>2+</sup>, the consequences of replacing Mg<sup>2+</sup> with Ca<sup>2+</sup> for Dpo4 activity have not been investigated to date. We show here that Ca<sup>2+</sup> (but not Ba<sup>2+</sup>, Co<sup>2+</sup>, Cu<sup>2+</sup>, Ni<sup>2+</sup>, or Zn<sup>2+</sup>) is a cofactor for Dpo4-catalyzed polymerization with both native and 8-oxoG-containing DNA templates. Both dNTP and ddNTP are substrates of the polymerase in the presence of either Mg<sup>2+</sup> or Ca<sup>2+</sup>. Conversely, no pyrophosphorolysis occurs in the presence of Ca<sup>2+</sup>, although the positions of the two catalytic metal ions at the active site appear to be very similar in mixed Mg<sup>2+</sup>/Ca<sup>2+</sup>- and Ca<sup>2+</sup>-form Dpo4 crystals.

DNA polymerases exhibit considerable sequence and structural diversity, but the catalytic cores in all of them share three subdomains: palm, thumb, and fingers (1). The palm harbors conserved acidic residues that coordinate two divalent metal ions required for catalysis (2). The fingers form interactions with the incoming nucleoside triphosphate, and residues from the thumb contact the minor groove of the DNA template–primer duplex. The so-called Y-class translesion polymerases possess an additional little finger or PAD domain (3, 4) that is crucial for damage sensing and bypass (5).

Considerable progress has been made in recent years with regard to our understanding of how both replicative and translesion DNA polymerases deal with damaged DNA (4, 6). Much of the structural information gained for the latter class stems from binary and ternary complexes with DNA of the Dpo4 DNA polymerase from *Sulfolobus solfataricus* (7–11). Although Dpo4 has served as a model system for eukaryotic polymerase  $\eta$ , there is some evidence for distinct mechanisms used by the two polymerases to bypass damage (12). Moreover, recent structural data and biochemical evidence support the notion that individual translesion polymerases appear to employ diverse mechanisms to replicate damaged DNA (13–15).

The 7,8-dihydro-8-oxodeoxyguanosine (8-oxoG) modification constitutes a challenge for replicative polymerases, and

most of them preferentially insert dA opposite 8-oxoG instead of dC (reviewed in ref 6). Conversely, DNA polymerase  $\eta$  is capable of bypassing 8-oxoG in a virtually error-free manner (16, 17). We have recently analyzed primer extension by Dpo4 opposite 8-oxoG-containing templates and found that the polymerase replicates the adduct with high fidelity (19:1 dC:dA ratio) (18). Inspection of crystal structures of ternary complexes between Dpo4 and primer–template constructs with either dATP, dCTP, ddCTP, dGTP, or ddGTP paired with 8-oxoG identified an arginine of the little finger (LF) domain at the origin of the strong preference for dC over dA (18). Arg332 hydrogen bonds to the 8-oxygen at the edge of the major groove with 8-oxoG adopting an anti conformation opposite (d)dCTP. When 8-oxoG flips to the syn conformation and pairs with dATP, no hydrogen bond exists between Arg332 and N3 of 8-oxoG. The structural data also provide a rationalization of the asymmetry in the efficiency of incorporation that differs strongly with Dpo4, depending on whether the 8-oxoG adduct is the templating base or the nucleoside triphosphate being incorporated.

Crystals grown with Dpo4, the 18mer template containing 8-oxoG, the 13mer primer, and either dCTP or ddCTP in the presence of calcium acetate unexpectedly revealed primers with single nucleotide extensions and (d)dCTP paired with 8-oxoG at the active site (18) (Figure 1). As with all other DNA polymerases, Mg<sup>2+</sup> and Mn<sup>2+</sup> are cofactors of Dpo4 (19, 20). Dpo4 also relies on pyrophosphorolysis for increasing the fidelity of replication (20). Although all crystals of Dpo4 complexes have been grown with Ca<sup>2+</sup>, a known inhibitor of many DNA polymerases (i.e., refs 21

<sup>†</sup> Supported in part by U.S. Public Health Service Grants R01 ES010375 and P30 ES000267, and P01 ES05355.

\* To whom correspondence should be addressed. Phone: (615) 343-8070. Fax: (615) 322-7122. E-mail: martin.egli@vanderbilt.edu.

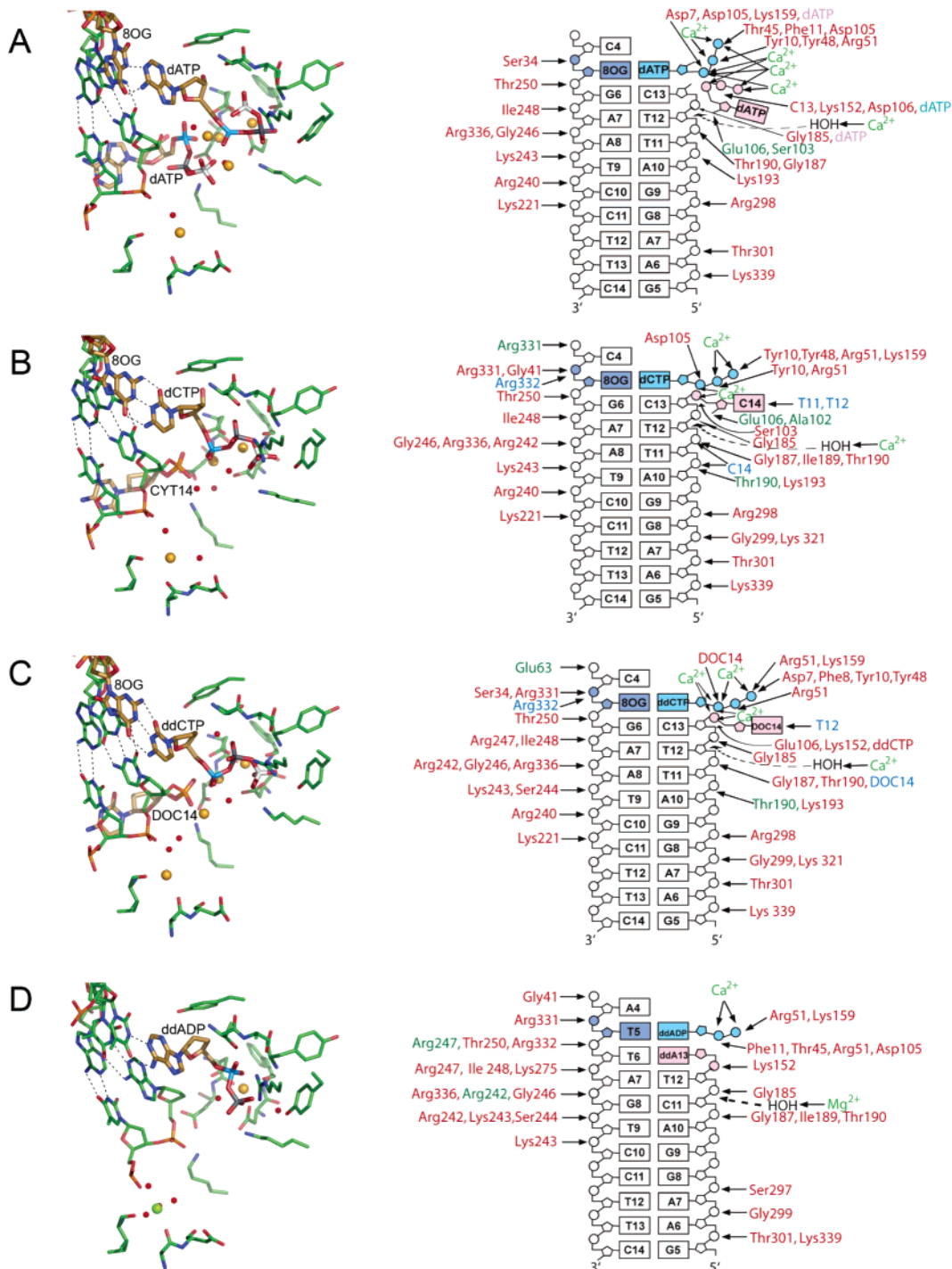


FIGURE 1: Metal ion coordination and conformations of the nucleoside triphosphate and primer–template duplex at the active sites of Dpo4 in crystal structures of type I ternary complexes (left panels). Schematic diagrams of the detailed intermolecular contacts and metal ion coordination modes in the individual Dpo4–DNA complexes (right panels). (A) Dpo4–dATP (PDB entry 2C2D), (B) Dpo4–dCTP (PDB entry 2C2E), and (C) Dpo4–ddCTP (PDB entry 2C2R) Ca<sup>2+</sup>-form complexes in which the NTP is paired to template 8-oxoG (8OG) (*I8*). (D) Mixed Mg<sup>2+</sup>/Ca<sup>2+</sup>-form complex with native DNA from ref 7 (PDB entry 1JX4). The 8-oxoG, the d(d)NTP, and the 14th nucleotide of the primer extended by polymerase (panels B and C only) are highlighted in light brown. Ca<sup>2+</sup> ions, Mg<sup>2+</sup> ions (Mg<sup>2+</sup> present in panel D only; however, the identity of the divalent ion cannot be taken for granted), and water molecules are spheres colored orange, green, and red, respectively. Residues interacting with metal ions or with d(d)NTP are colored by atom type with carbon atoms colored green. Template–primer base pair hydrogen bonds are shown as thin dashed lines.

and 22), no data regarding the effects of Ca<sup>2+</sup> on Dpo4 activity have been published to our knowledge. The observation of extended primers in crystals of Dpo4–DNA complexes obtained in the presence of Ca<sup>2+</sup> but in the absence of Mg<sup>2+</sup> (*I8*) prompted us to assay Dpo4 activity with Ca<sup>2+</sup>. Here we show that although Ca<sup>2+</sup> is not the preferred divalent metal ion, it acts as a cofactor of Dpo4-catalyzed polymer-

ization. Conversely, Ca<sup>2+</sup> is an inhibitor of the pyrophosphorolysis activity of Dpo4. The different roles played by Mg<sup>2+</sup> and Ca<sup>2+</sup> are unlikely to be a consequence of changes in the positions of the two catalytic metal ions at the Dpo4 active site but rather appear to be related to the preferred modes of interactions of individual alkaline earth metal ions with the primer–template duplex.

## MATERIALS AND METHODS

**Reagents.** Dpo4 was expressed in *Escherichia coli* and purified using heat denaturation, Ni<sup>2+</sup>-nitriloacetate chromatography, and ion-exchange chromatography as described elsewhere (18). All oligonucleotides used in this work were synthesized by Midland Certified Reagent Co. (Midland, TX) and purified by HPLC by the manufacturer, with analysis by matrix-assisted laser desorption time-of-flight MS.

**Calcium Concentration Effect in Primer Extension Assays Using All Four dNTPs.** To avoid activity due to trace metal ion contaminations (i.e., Mg<sup>2+</sup>) in the primer extension reactions, double-distilled water and solutions of Tris buffer and NaCl (8–10 mL each) were treated with 0.5 g of Chelex 100 ion-exchange resin (Bio-Rad Laboratories, Hercules, CA) (23). The suspensions were gently stirred at room temperature for 1 h, followed by centrifugation. The supernatants were decanted and centrifuged before being used. All the polymerization reaction mixtures were incubated in Teflon film-lined Eppendorf tubes to prevent contaminations from containers. Each reaction was initiated by adding 2  $\mu$ L of a dNTP solution (final concentrations of 1 mM of each dNTP and different concentrations of MgCl<sub>2</sub> or CaCl<sub>2</sub>) to a preincubated E·DNA complex [final concentrations of 50 mM Tris-HCl (pH 7.8), 1  $\mu$ M DNA duplex, 1.5  $\mu$ M Dpo4, 2 mM DTT, 100  $\mu$ g/mL BSA, 50 mM NaCl, and 2% glycerol (v/v)] at 37 °C, yielding a total reaction volume of 20  $\mu$ L. After 0.5 h, reactions were quenched with 100  $\mu$ L of 20 mM EDTA (pH 9.0) in 95% formamide (v/v). Aliquots (3  $\mu$ L) were separated by electrophoresis using denaturing gels containing 8.0 M urea and 16% acrylamide (w/v) [from a 19:1 acrylamide/bisacrylamide solution (w/w), AccuGel, National Diagnostics, Atlanta, GA] with 80 mM Tris-borate buffer (pH 7.8) containing 1 mM EDTA. The gel was exposed to a phosphorimager screen (Imaging Screen K, Bio-Rad) overnight. The bands (representing extension of the primer) were visualized with a phosphorimaging system (Molecular Imager FX, Bio-Rad) using the manufacturer's Quantity One software, version 4.3.0. Concentration effects for other metal ions (Ba<sup>2+</sup>, Co<sup>2+</sup>, Cu<sup>2+</sup>, Mn<sup>2+</sup>, Ni<sup>2+</sup>, Sr<sup>2+</sup>, and Zn<sup>2+</sup>) were analyzed in an analogous fashion.

**Single-Step Primer Extension Assays and Gel Electrophoresis.** A <sup>32</sup>P-labeled primer, annealed to either an unmodified or 8-oxoG template, was extended in the presence of the individual dNTPs or ddNTPs. Each reaction was initiated by adding 2  $\mu$ L of a dNTP or ddNTPs solution (final concentrations of 1 mM for each dNTP and 10 mM MgCl<sub>2</sub> or CaCl<sub>2</sub>) to a preincubated E·DNA complex (see above for final concentrations) at 25 °C, yielding a total reaction volume of 6  $\mu$ L. After 2, 10, and 25 h (2, 5, and 10 min for Mg<sup>2+</sup>-bound dNTP), reactions were quenched with 500  $\mu$ L of 20 mM EDTA (pH 9.0) in 95% formamide (v/v). Aliquots (3  $\mu$ L) were separated by electrophoresis using denaturing gels as described above.

**Primer Extension Assays Using All Four dNTPs.** A <sup>32</sup>P-labeled 13-mer primer, annealed to either an unmodified or 8-oxoG template, was extended in the presence of the four dNTPs. Each reaction was initiated by adding 2  $\mu$ L of a dNTP solution (final concentrations of 1 mM for each dNTP and 10 mM MgCl<sub>2</sub> or CaCl<sub>2</sub>) to a preincubated E·DNA complex (see above for final concentrations) at 37 °C, yielding a total reaction volume of 10  $\mu$ L. After 0.5, 1, and

16 h, reactions were quenched with 100  $\mu$ L of 20 mM EDTA (pH 9.0) in 95% formamide (v/v). Aliquots (3  $\mu$ L) were separated by electrophoresis using denaturing gels as described above.

**Steady-State Kinetic Assays.** A <sup>32</sup>P-labeled 13-mer primer, annealed to either an unmodified or 8-oxoG template, was extended in the presence of dCTP. Each reaction was initiated by adding 2  $\mu$ L of a dCTP solution (0.5–1000  $\mu$ M) to a preincubated E·DNA complex [final concentrations of 50 mM Tris-HCl (pH 7.8), 100 nM DNA duplex, 50 nM Dpo4, 2 mM DTT, 100  $\mu$ g/mL BSA, 50 mM NaCl, 2% glycerol (v/v), and 5 mM CaCl<sub>2</sub>] at 37 °C, yielding a total reaction volume of 10  $\mu$ L. After 15 min, reactions were quenched with 100  $\mu$ L of 20 mM EDTA (pH 9.0) in 95% formamide (v/v). Aliquots (3  $\mu$ L) were separated by electrophoresis using denaturing gels as described above.

**Dpo4-Catalyzed Pyrophosphorolysis.** A DNA template with a 14-mer primer (100 nM, C opposite unmodified G or 8-oxoG) was preincubated at room temperature for 5 min with Dpo4 (150 nM) in a reaction mixture (8  $\mu$ L) containing 50 mM Tris (pH 7.8), 10 mM DTT, 200  $\mu$ g/mL BSA, 2.5% glycerol, and 5 mM MgCl<sub>2</sub> or CaCl<sub>2</sub> to allow the formation of the polymerase–DNA binary complex. Pyrophosphorolysis was then initiated by the addition of various concentrations of PP<sub>i</sub> without dNTPs. After 3 min at 60 °C, the reactions were quenched with 100  $\mu$ L of 20 mM EDTA (pH 9.0) in 95% formamide (v/v) and analyzed on a 16% polyacrylamide–8 M urea sequencing gel. The primer degradation bands were visualized with a phosphorimaging system as described above.

## RESULTS

**Active Site Properties of Dpo4 Based on Crystallographic Data.** Compared to those of other translesion polymerases, the structure and function of Dpo4 DNA polymerase from *S. solfataricus* have been studied in particular detail. Crystal structures of ternary complexes have disclosed two different arrangements of the primer–template duplex at the active site. In the type I form, only the replicating template base and the incoming dNTP are accommodated at the active site, whereas two template bases reside in the more open binding pocket of type II complexes (7). The reported crystallization conditions for Dpo4 complexes vary only minimally; typically, protein and DNA are annealed in the presence of either 5 mM Mg<sup>2+</sup> or Ca<sup>2+</sup>, and this mixture is then combined with a solution containing 100 mM calcium acetate for growing crystals (7). Two orthorhombic crystal forms have been observed, one featuring a single Dpo4–DNA complex per asymmetric unit (i.e., refs 7 and 18) and the other two independent complex molecules (i.e., refs 10 and 20). Crystals of binary Dpo4–DNA complexes can also be grown from magnesium acetate but diffract X-rays only poorly (our unpublished data). In cases where crystals were grown using both Mg<sup>2+</sup> and Ca<sup>2+</sup> ions (in the annealing and reservoir solutions, respectively), it is difficult to establish the nature of metal ions identified in the structure. Although divalent ions at the active site were treated as Mg<sup>2+</sup> in some structures, probably due to the regular octahedral coordination geometry typical for Mg<sup>2+</sup> (i.e., ref 20), it remains possible that high concentrations of calcium acetate caused displacement of Mg<sup>2+</sup>. Recently, diffraction data for Dpo4–

DNA complex crystals were collected at longer X-ray wavelengths to distinguish between  $Mg^{2+}$  and  $Ca^{2+}$  on the basis of their different contributions to anomalous scattering (24). This work demonstrated that all ions present at and adjacent to the active sites of the complexes were  $Ca^{2+}$ . By analogy, we can infer that the ions in the original type I ternary complex with ddATP are also  $Ca^{2+}$  (7). These crystals were grown from 100 mM calcium acetate following in situ extension of the 12-mer primer in the presence of 1 mM ddATP and 5 mM magnesium chloride.

Calcium is usually expected to inhibit extension of the primer during crystallization of polymerase–DNA–dNTP complexes, but in addition, a 2',3'-dideoxynucleotide is often used at the 3'-terminus of the primer to prevent polymerization (i.e., refs 7 and 13). In recent crystal structures of type I complexes of Dpo4 with 18-mer template DNA containing an 8-oxoG lesion, a 13-mer primer (2'-deoxynucleotide at the 3'-terminus), either dCTP or ddCTP, and  $Ca^{2+}$  only (no  $Mg^{2+}$ ), we found that the primer had been extended by (d)dC and a further (d)dCTP paired to template 8-oxoG (18) (Figure 1B,C). Thus, neither  $Ca^{2+}$  nor the use of a dideoxynucleoside triphosphate (nor both) appeared to have prevented extension of the primer. Analysis of primer extension by Dpo4 opposite 8-oxoG with  $Mg^{2+}$  demonstrated >95% incorporation of dCTP over dATP, contrary to the observations with this lesion for the majority of DNA polymerases (18 and references cited therein). Consistent with the kinetic data in the presence of  $Mg^{2+}$  that show dATP to be a poorer substrate opposite 8-oxoG than dCTP [ $k_{cat}/K_m$  values of  $0.22 \pm 0.04$  and  $0.0075 \pm 0.0004 \text{ min}^{-1} \mu\text{M}^{-1}$ , respectively (18)], the crystal structure of the complex with dATP revealed an unextended primer and two nucleoside triphosphate molecules at the active site (Figure 1A). Crystal structures of type II complexes with an unpaired 8-oxoG and the 5'-tC paired to either dGTP or ddGTP at the active sites (Figure S1A,B of the Supporting Information) also contained 13-mer primers, indicating that  $Ca^{2+}$  may be unable to act as a cofactor for lesion bypass involving frameshifts.

In the Dpo4–dCTP and Dpo4–ddCTP complexes with single-nucleotide extensions, the 3'-terminal hydroxyl group of the primer is relatively far removed from the  $\alpha$ -phosphate of the (d)dCTP because of a sharp turn in the primer that places the terminal (d)dC in the minor groove (Figure 1B,C). Because these complexes were annealed and crystallized in the presence of  $Ca^{2+}$  only, the identity of the electron density peaks assigned to divalent ions is not in question. Other than the fact that more than two metal ions are present at the active sites of the complexes depicted in panels A–C Figure 1, the geometry of the binding pocket and the conformation of the template strand differ only minimally from those seen in the structure of the ternary complex of Dpo4 with native DNA (Figure 1D). Motivated by the crystallographic data, we first analyzed the role of  $Ca^{2+}$  as a potential cofactor for Dpo4-catalyzed DNA polymerization.

**Effect of Calcium Concentration on the Polymerase Activity.** Because  $Ca^{2+}$  is a common inhibitor of DNA polymerases and to address the question of whether the primer extensions seen in the crystal structures of ternary Dpo4–DNA–(d)dCTP complexes were possibly due to trace amounts of  $Mg^{2+}$  (from either Dpo4, buffer components, glassware, or plasticware), we assayed extensions of a 13-mer primer in the presence of all four dNTPs and various

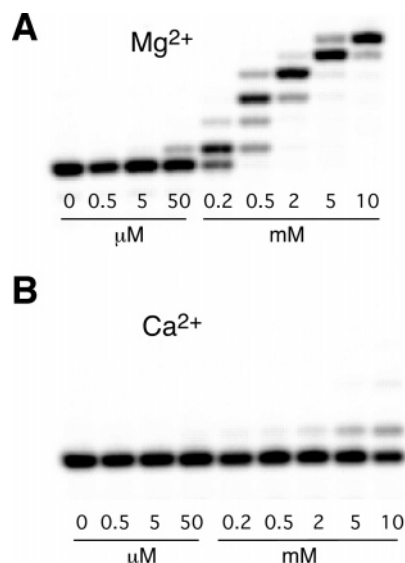


FIGURE 2: Effect of calcium concentration on the extension of a DNA primer by Dpo4 with all four dNTPs. Extension of the  $^{32}\text{P}$ -labeled 13-mer primer 5'-GGG GGA AGG ATT C-3' opposite the 18-mer template 3'-CCC CCT TCC TAA GGC ACT-5' in the presence of increasing concentrations (indicated) of (A)  $Mg^{2+}$  or (B)  $Ca^{2+}$  was analyzed at 37 °C after 30 min. The longer primer products that formed in the presence of 5 and 10 mM  $Mg^{2+}$  are the result of blunt end extensions off the full-length product.

amounts of either  $Mg^{2+}$  or  $Ca^{2+}$  (Figure 2; see the figure legend for the sequence of the primer–template construct). Teflon-coated containers rather than regular glassware and plasticware were used for investigating metal ion effects. Double-distilled water was used for the enzymatic reactions, and buffer solutions were treated with Chelex 100 ion-exchange resin. From the gel depicted in Figure 2A, it is apparent that  $Mg^{2+}$  concentrations of either 0.5 or 5  $\mu\text{M}$  do not result in any polymerization activity. Trace amounts of  $Mg^{2+}$  are indeed universal in  $CaCl_2$  samples. The calculated concentration of  $Mg^{2+}$  in the 10 mM  $CaCl_2$  solution is 0.25  $\mu\text{M}$  on the basis of the information provided by the producer on the label of the  $CaCl_2$  container. Since polymerase activity is observed at  $Ca^{2+}$  concentrations well below 10 mM (Figure 2B),  $Mg^{2+}$  contamination cannot be the cause of the activity. Without the addition of a divalent metal cation, no extension is observed (Figure 2). Therefore, traces of  $Mg^{2+}$  potentially present in the enzyme following purification cannot be the reason for the extension seen with  $Ca^{2+}$ . More importantly, there is a clear concentration dependence of the  $Ca^{2+}$  activity (Figure 2B). The activity gradually increases when the concentration of  $Ca^{2+}$  is increased with initial activity visible at 0.2 mM  $Ca^{2+}$ . Therefore, these assays provide evidence that contradicts the contamination hypothesis. Similarly, we tested polymerase activity in the presence of increasing concentrations of  $Ba^{2+}$ ,  $Co^{2+}$ ,  $Cu^{2+}$ ,  $Mn^{2+}$ ,  $Ni^{2+}$ ,  $Sr^{2+}$ , and  $Zn^{2+}$  (Figure S2). With the exception of  $Mn^{2+}$  (20), none of these metal ions act as cofactors. However,  $Mn^{2+}$  contamination of  $CaCl_2$  cannot account for the polymerase activity seen with  $Ca^{2+}$ .

**Single-Nucleotide Extensions and Steady-State Kinetics.** Extension of a 13-mer primer opposite G in an 18-mer template was assayed separately for all four dNTPs and ddNTPs in the presence of  $Ca^{2+}$ , using the corresponding extensions with  $Mg^{2+}$  as a reference (Figure 3; see the figure legend for the sequence of the primer–template construct).

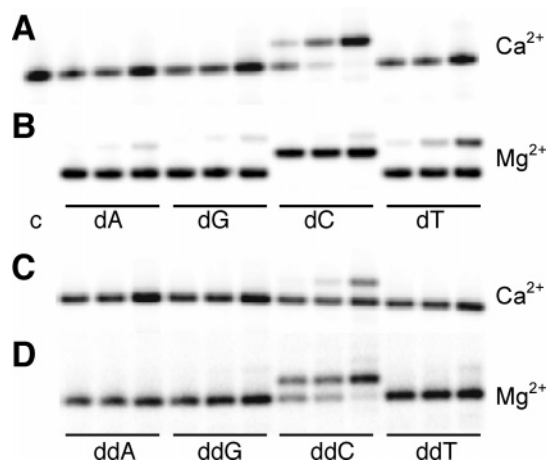


FIGURE 3: Metal ion dependence of single-base extension of a DNA primer by Dpo4. Extension of the  $^{32}\text{P}$ -labeled 13-mer primer 5'-GGG GGA AGG ATT C-3' opposite G (bold) of the 18-mer template 3'-CCC CCT TCC TAA GGC ACT-5' in the presence of (A)  $\text{Ca}^{2+}$  and dNTP, (B)  $\text{Mg}^{2+}$  and dNTP, (C)  $\text{Ca}^{2+}$  and ddNTP, and (D)  $\text{Mg}^{2+}$  and ddNTP was analyzed at 25 °C with increasing reaction times (2, 10, and 25 h; (B) 2, 5, and 10 min; c is control).

Table 1: Steady-State Kinetic Parameters for Single-Base Extension Reactions by Dpo4 in the Presence of either  $\text{Ca}^{2+}$  or  $\text{Mg}^{2+}$

18-mer template with a 13-mer primer substrate	G-bound dCTP	8-oxoG-bound dCTP
$k_{\text{cat}}(\text{Ca}^{2+})$ ( $\text{min}^{-1}$ )	$0.022 \pm 0.001$	$0.049 \pm 0.001$
$k_{\text{cat}}(\text{Mg}^{2+})$ ( $\text{min}^{-1}$ ) <sup>a</sup>	$0.83 \pm 0.02$	$0.24 \pm 0.01$
$K_{\text{m,dCTP}}(\text{Ca}^{2+})$ (mM)	$0.54 \pm 0.1$	$0.54 \pm 0.1$
$K_{\text{m,dCTP}}(\text{Mg}^{2+})$ (mM) <sup>a</sup>	$6.5 \pm 0.9$	$1.1 \pm 0.02$
$k_{\text{cat}}/K_{\text{m}}(\text{Ca}^{2+})$ ( $\text{min}^{-1} \text{mM}^{-1}$ )	$0.04 \pm 0.01$	$0.09 \pm 0.01$
$k_{\text{cat}}/K_{\text{m}}(\text{Mg}^{2+})$ ( $\text{min}^{-1} \text{mM}^{-1}$ ) <sup>a</sup>	$0.13 \pm 0.02$	$0.22 \pm 0.04$

<sup>a</sup> From ref 18.

As expected, only dC and ddC are inserted, the latter with clearly diminished efficiency. The extent of insertion of dCTP with  $\text{Ca}^{2+}$  is comparable to that for insertion of ddCTP with  $\text{Mg}^{2+}$  (Figure 3A,D). Steady-state kinetic parameters for  $\text{Ca}^{2+}$ - and  $\text{Mg}^{2+}$ -dependent extensions by dCTP opposite either G or 8-oxoG in the same sequence context are listed in Table 1. From the data, it is apparent that Dpo4 activity is considerably reduced with  $\text{Ca}^{2+}$  as a cofactor (ca. 40-fold for  $k_{\text{cat}}$  and ca. 3-fold for  $k_{\text{cat}}/K_{\text{m}}$ ). Single-extension assays conducted with a template containing 8-oxoG reveal that dCTP is somewhat preferred over dATP with  $\text{Ca}^{2+}$  (Figure S3). Again, the efficiency is comparable to that in the presence of  $\text{Mg}^{2+}$  with ddNTPs, although ddC is clearly preferred over ddA with  $\text{Mg}^{2+}$  (Figure S3A,C). Thus, the base selectivities observed with the two metal ions exhibit similar trends, but the level of misincorporation (i.e., dT opposite G or 8-oxoG; Figures 3 and S3) is clearly diminished with  $\text{Ca}^{2+}$  due to the lower overall efficiency of polymerization.

**Full-Length Extension of a Primer in the Presence of All Four dNTPs.** Next we tested whether the 13-mer primer could be extended to the full-length product using all four nucleoside triphosphates. This assay was conducted with the same 18-mer template sequences that were used in the previous single-base extension experiments. As shown in Figure 4, the activity of Dpo4 is significantly reduced with the  $\text{Ca}^{2+}$  cofactor compared to that with  $\text{Mg}^{2+}$ . Whereas synthesis of the full-length product is completed long before

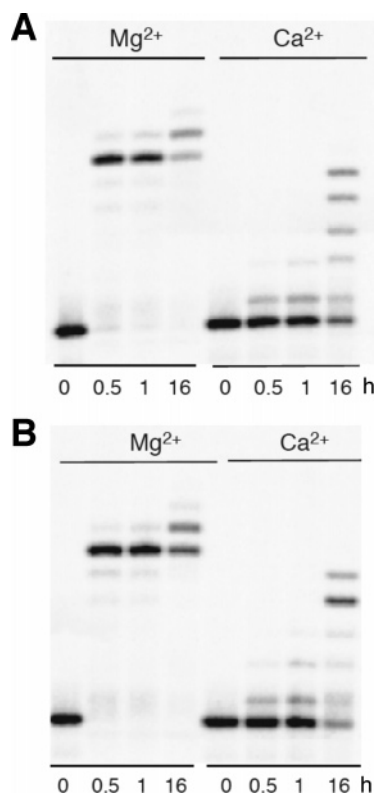


FIGURE 4: Metal ion dependence of extension of a DNA primer by Dpo4 with all four dNTPs. Extension of the  $^{32}\text{P}$ -labeled 13-mer primer 5'-GGG GGA AGG ATT C-3' opposite the 18-mer template 3'-CCC CCT TCC TAA GXC ACT-5' [ $\text{X} = \text{G}$  (A) or 8-oxoG (B)] in the presence all four dNTPs and either  $\text{Ca}^{2+}$  or  $\text{Mg}^{2+}$  was analyzed at 37 °C with increasing reaction times (indicated). The longer primer products that formed in the presence of  $\text{Mg}^{2+}$  are the result of blunt end extensions of the full-length product.

the first time point (30 min) with  $\text{Mg}^{2+}$ , only a small fraction of the extended sequences is constituted by the 18-mer in the presence of  $\text{Ca}^{2+}$  even after 16 h. The results of the extensions with the native DNA and 8-oxoG-containing templates are qualitatively the same. As indicated by the results of the single-base extension assays before,  $\text{Ca}^{2+}$  is not as good a cofactor as  $\text{Mg}^{2+}$  but clearly not an inhibitor of the Dpo4 polymerase activity as it allows formation of the full-length product.

**Metal Ion Dependence of Pyrophosphorolysis.** The ability of Dpo4 to promote pyrophosphorolysis that reverses the polymerization reaction was also tested in the presence of  $\text{Mg}^{2+}$  and  $\text{Ca}^{2+}$ . Unlike related translesion polymerases, Dpo4 has robust pyrophosphorolysis activity in the presence of pyrophosphate ( $\text{PP}_i$ ) and  $\text{Mg}^{2+}$  (20) (Figure 5). Pyrophosphorolysis may allow Dpo4 to increase the fidelity by stalling mispaired primer extension. Interestingly,  $\text{Ca}^{2+}$  inhibits pyrophosphorolysis as there is no shortening of the 14-mer primer apparent in the assays conducted with both native DNA and 8-oxoG-modified 18-mer templates (Figure 5).

## DISCUSSION

Magnesium is generally believed to be the divalent metal ion utilized by most polymerases for catalysis in vivo (25). DNA polymerases appear to be inhibited by  $\text{Ca}^{2+}$ , although reports of the precise nature of changes at the active sites of DNA polymerases as a result of the presence of different mono- or divalent metal ions are rare (21, 22).  $\text{Ca}^{2+}$  has a

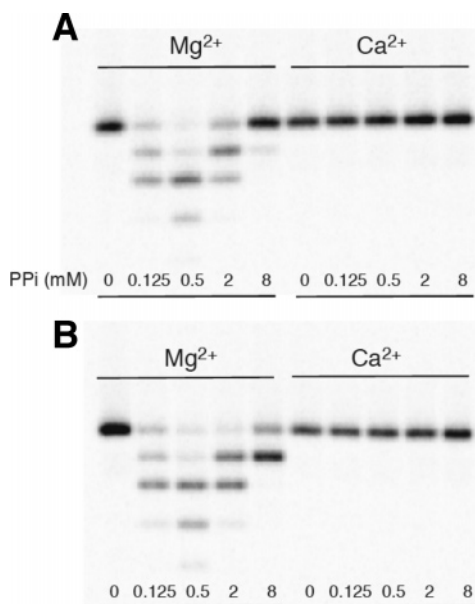


FIGURE 5: Metal ion dependence of pyrophosphorolysis by Dpo4. Pyrophosphorolysis of the  $^{32}\text{P}$ -labeled 14-mer primer 5'-GGG GGA AGG ATT CC-3' opposite the 18-mer template 3'-CCC CCT TCC TAA GXC ACT-5' [X = G (A) or 8-oxoG (B)] in the presence of either  $\text{Ca}^{2+}$  or  $\text{Mg}^{2+}$  and increasing amounts of  $\text{PP}_i$  (indicated) without dNTPs was analyzed at 60 °C.

larger ionic radius than  $\text{Mg}^{2+}$  (0.90 and 0.65 Å, respectively), rendering the former less effective in polarizing the P–O bond for nucleophilic attack.  $\text{Ca}^{2+}$  also differs from  $\text{Mg}^{2+}$  in terms of its coordination chemistry. A search in the metallo-protein database (26) reveals that a regular octahedral coordination mode of  $\text{Mg}^{2+}$  is most common whereas the  $\text{Ca}^{2+}$  coordination mode is more variable, with frequent occurrences of ions surrounded by four to eight ligands (data not shown). Further differences between the two ions concern hydration enthalpy [–1921 and –1577 kJ/mol for  $\text{Mg}^{2+}$  and  $\text{Ca}^{2+}$ , respectively (27)], resulting in facilitated inner-sphere coordination of  $\text{Ca}^{2+}$  to DNA (28), and the  $\text{pK}_a$  of a water molecule coordinated to  $\text{Mg}^{2+}$  (11.4) or  $\text{Ca}^{2+}$  (12.8) (29, 30). Detailed studies based on crystals of human pol  $\beta$  soaked in various metal ions revealed that  $\text{Ca}^{2+}$  and other ions coordinate the triphosphate moiety of (d)dNTP in a manner different from that of  $\text{Mg}^{2+}$  and also promote a change in the side chain conformation of one of the three highly conserved active site carboxylate residues involved in metal ion binding (21). However,  $\text{Ca}^{2+}$  is commonly used alone or in combination with a 2',3'-dideoxynucleotide at the primer terminus to prevent polymerization under crystallization conditions (i.e., ref 7).

Our crystal structures of Dpo4–DNA–(d)dCTP complexes with 8-oxoG in the template obtained under  $\text{Ca}^{2+}$ -only conditions (Figure 1) (18) and in vitro primer extensions assaying the dependence of Dpo4 polymerase activity on the concentration of  $\text{Mg}^{2+}$  or  $\text{Ca}^{2+}$  (Figure 2) prove unambiguously that  $\text{Ca}^{2+}$  promotes polymerization. In vitro single-nucleotide and full-length primer extension analyses confirm that  $\text{Ca}^{2+}$  is a cofactor of polymerase activity (Figures 3, 4, and S3). However, the kinetic data show that with both native and 8-oxoG-modified templates Dpo4 performs more poorly in the presence of  $\text{Ca}^{2+}$  than in the presence of  $\text{Mg}^{2+}$  (Table 1). The extent of product formation with the natural dNTP substrates and  $\text{Ca}^{2+}$  is comparable to that with ddNTPs and

$\text{Mg}^{2+}$  (Figure 3).

Do the crystallographic data provide insight with regard to the differences in the catalytic efficiencies of Dpo4 with either  $\text{Mg}^{2+}$  or  $\text{Ca}^{2+}$  as a cofactor? One complicating factor is the fact that there is probably no pure  $\text{Mg}^{2+}$ -form crystal structure of a Dpo4–DNA complex available ( $\text{Mg}^{2+}$  occupying both active site positions), as crystals for all structures reported to date were grown either in the presence of both metal ions [with an excess of  $\text{Ca}^{2+}$  (i.e., refs 7, 11, and 20)] or with  $\text{Ca}^{2+}$  alone (i.e., refs 11 and 18). Structures of mixed  $\text{Mg}^{2+}/\text{Ca}^{2+}$ -form and  $\text{Ca}^{2+}$ -form complexes reveal virtually no changes in the location and coordination of the two metal ions at the active site (11). The orientation of the triphosphate moiety displays some variation (Figure 1A,B) (11, 20); however, the location of metal ions appears to be unaffected by these conformational differences, and they are unlikely to be the result of the particular divalent ion used in the crystallizations. Thus, the Dpo4–dATP and Dpo4–dCTP structures (panels A and B of Figure 1, respectively) were both obtained in the presence of  $\text{Ca}^{2+}$  but exhibit different orientations of the  $\beta$ - and  $\gamma$ -phosphate groups. By comparison, dNTPs and ddNTPs bind differently at the Dpo4 active site with the 3'-hydroxyl group of the former engaging in a hydrogen bond to the main chain nitrogen of Tyr12 that is absent with ddNTPs (11) (Figure S1). Clearly, this slight misalignment is the chief reason for the reduced activity of Dpo4 with ddNTPs relative to dNTPs in the single-nucleotide extensions assayed with both  $\text{Ca}^{2+}$  and  $\text{Mg}^{2+}$  (Figures 3 and S3). The structure of a binary Dpo4 complex as a result of a single-nucleotide extension following annealing with  $\text{Mg}^{2+}$  and crystallization with  $\text{Ca}^{2+}$  reveals a shift of one of the two divalent ions present at the active site compared with other structures (20) (Figure 6). However, this shift is unlikely to be relevant in explaining the different efficiencies seen with  $\text{Mg}^{2+}$  and  $\text{Ca}^{2+}$  and is likely the result of a lack of a nucleoside triphosphate whose place is taken by dG and  $\text{PP}_i$  instead. Even in this structure, it is unclear whether the shifted ion is actually  $\text{Mg}^{2+}$  (Figure 6); there remains a possibility that both ions seen at the active site are actually  $\text{Ca}^{2+}$ .

One intriguing observation with respect to the structures of the  $\text{Ca}^{2+}$ -form Dpo4–dCTP and –ddCTP complexes with extended primers and the Dpo4–dATP complex is the presence of a second nucleoside triphosphate (Figures 1 and 6). Instead of a primer–template duplex shifted into the –1 position following replication and the following template base paired to (d)dNTP, the crystals have trapped an arrangement whereby the added nucleotide is looped out, thus allowing pairing of the next nucleotide substrate to 8-oxoG. Although the conformation of the primer would obviously render impossible further extension, the in vitro data in the presence of all four dNTPs demonstrate that the full-length product is still produced with  $\text{Ca}^{2+}$  as the cofactor (Figure 4). The polymerization state trapped in the crystals, although it may not be representative of an intermediate of the in vitro reaction with  $\text{Ca}^{2+}$  (11), sheds nevertheless light on potential differences in the manners in which  $\text{Mg}^{2+}$  and  $\text{Ca}^{2+}$  interact with the primer–template duplex. The disruption of the replicated base pair in the  $\text{Ca}^{2+}$  structures with 8-oxoG-containing templates is the most obvious difference from all other structures reported for Dpo4 complexes. In addition, between one and three additional metal ions are

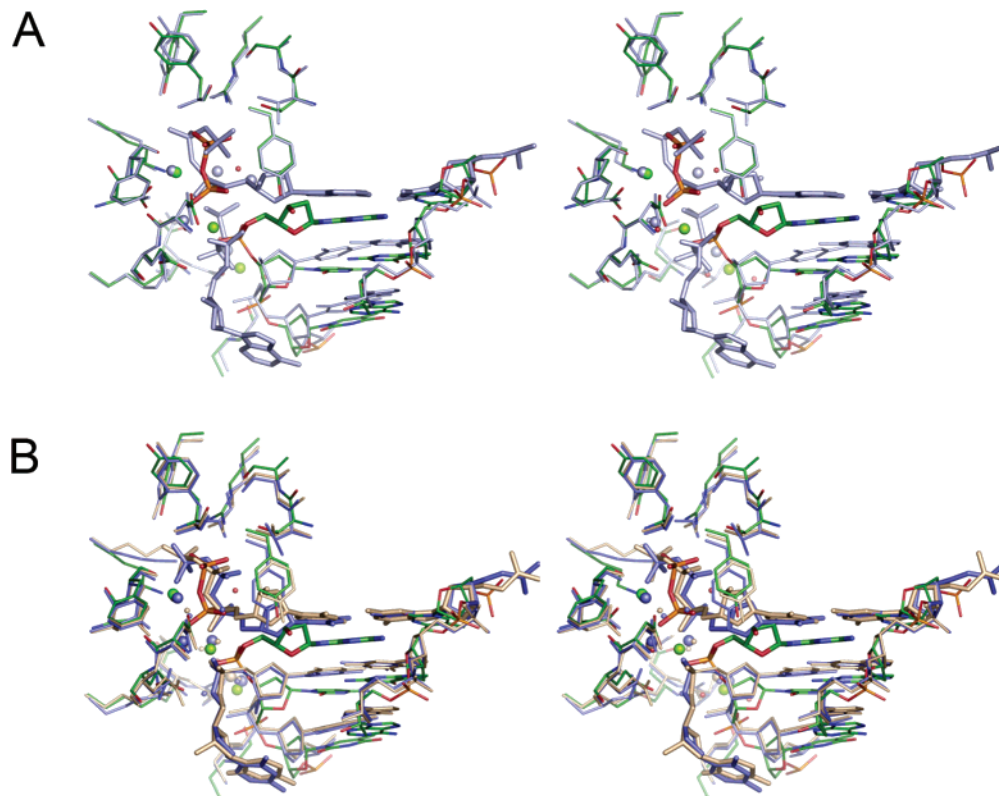


FIGURE 6: Comparison between the active sites in  $\text{Ca}^{2+}$ - and mixed  $\text{Mg}^{2+}/\text{Ca}^{2+}$ -form Dpo4–DNA complexes. (A) Stereoview of a superimposition of the Dpo4–dATP ternary  $\text{Ca}^{2+}$ -form complex (PDB entry 2C2D) (18) and a binary  $\text{Mg}^{2+}/\text{Ca}^{2+}$ -form complex (PDB entry 2AGP) (20). The ternary complex features a dATP•8-oxoG pair at the active site, and bonds and  $\text{Ca}^{2+}$  ions are colored light blue. The binary complex features a pG•tT pair at the active site and is colored by atom with carbon atoms in green and divalent metal ions, either  $\text{Ca}^{2+}$  or  $\text{Mg}^{2+}$ , depicted as green spheres. (B) Stereoview of a superimposition of the Dpo4–dCTP (beige) and Dpo4–ddCTP (blue) ternary  $\text{Ca}^{2+}$ -form complexes (PDB entries 2C2E and 2C2R, respectively) (18) and the above binary  $\text{Mg}^{2+}/\text{Ca}^{2+}$ -form complex (color code identical to that in panel A).

present at and near the active site, undoubtedly helping to stabilize the increased number of negative charges due to the presence of a second nucleoside triphosphate molecule (Figures 1 and 6).

Interestingly, crystal structures of a B-form DNA dodecamer obtained with either  $\text{Mg}^{2+}$  or  $\text{Ca}^{2+}$  also revealed melted terminal base pairs in the  $\text{Ca}^{2+}$  form and looped-out residues residing in the minor groove (28). Although the DNA environments are quite different in the two cases, complexed with the polymerase here and packed against neighboring DNA molecules in the DNA crystals, the comparison is instructive in that it provides an indication of the structural polymorphism produced solely as a result of switching from one type of divalent ion to another. At the very least, the unique conformations of the DNA in the presence of  $\text{Ca}^{2+}$  at the Dpo4 active site observed in our complexes (Figure 1) point to divergent interactions with the primer–template duplex as one of the reasons for the different polymerization efficiencies elicited by  $\text{Mg}^{2+}$  and  $\text{Ca}^{2+}$ . By comparison, there are no actual data for Dpo4 that would support the notion that different coordination geometries or orientations of the two catalytic metal ions at the active site are the main reason for the different efficiencies seen with the two divalent metal ions. The crystal structures of the Dpo4–dCTP and –ddCTP complexes with extended primers appear to be consistent with 8-oxoG acting as a template twice. However, the results of the full-length primer extensions do not support this view (Figure 4). Crystallographic data can be overinterpreted, and further biochemical and kinetic data sometimes require one

to revisit earlier conclusions based solely on structural data. A case in point is the new evidence for Watson–Crick and not Hoogsteen pairing in the selection of nucleotides for insertion opposite the second residue of a thymidine dimer (12, 31), contradicting earlier conclusions based on crystal structures (8).

Calcium is an inhibitor of the pyrophosphorolysis activity of Dpo4 (Figure 5). The crystal structure of a mixed  $\text{Mg}^{2+}/\text{Ca}^{2+}$ -form binary Dpo4–DNA complex obtained with a single extension of the primer revealed a trapped  $\text{PP}_i$  molecule (20) (Figure 6). Conversely, our structures of ternary complexes with single extensions obtained in the presence of  $\text{Ca}^{2+}$  reveal an additional nucleotide instead. Although it remains difficult to ascertain the identity of divalent ions in crystals grown in the presence of both ions (vide supra), the structural data once more appear to support different preferences with regard to the interactions of  $\text{Mg}^{2+}$  and  $\text{Ca}^{2+}$  with the primer–template duplex and phosphate groups of either nucleotide or  $\text{PP}_i$  at the Dpo4 active site. The inhibitory effect of  $\text{Ca}^{2+}$  on the pyrophosphorolysis activity may be related to different relative affinities for  $\text{PP}_i$  and dNTP compared to that of  $\text{Mg}^{2+}$  and therefore facilitated removal of pyrophosphate. Thus, pyrophosphate is known to form highly insoluble precipitates with  $\text{Ca}^{2+}$  whose solubility is affected by a number of factors, including  $\text{Mg}^{2+}$  concentration and pH (32), and can be dissolved by enzymes such as alkaline phosphatase whose pyrophosphatase activity depends on  $\text{Mg}^{2+}$  (33). Under the conditions of the assay used here, there may simply not have been enough free  $\text{PP}_i$

available at the Dpo4 active site in the presence of  $\text{Ca}^{2+}$  to promote reversal of polymerization. This conclusion is supported by the observation that pyrophosphorolysis activity is markedly reduced when the  $\text{PP}_i$  concentration exceeds 2 mM in the assays with  $\text{Mg}^{2+}$  as the divalent ion is then depleted (Figure 5, left panels) (20).

In conclusion, we show preferential actions of divalent metal cations in the same row of the periodic table in two activities of an enzyme, even though these metals appear to occupy the same sites in the enzyme. This difference has implications for the interpretation of structural studies in the context of enzyme function.

## ACKNOWLEDGMENT

We thank Dr. Jeong-Yun Choi and Karen C. Angel for help with Dpo4 expression and purification.

## SUPPORTING INFORMATION AVAILABLE

Illustrations of metal ion coordination, conformations of nucleoside triphosphate and primer–template duplex and protein–DNA interactions at the active sites of Dpo4 type II ternary complexes, and metal ion dependence of extensions of a 13-mer primer opposite native and 8-oxoG-containing 18-mer templates. This material is available free of charge via the Internet at <http://pubs.acs.org>.

## REFERENCES

- Steitz, T. A. (1993) DNA- and RNA-dependent DNA polymerases, *Curr. Opin. Struct. Biol.* 3, 31–38.
- Steitz, T. A. (1993) DNA polymerases: Structural diversity and common mechanisms, *J. Biol. Chem.* 274, 17395–17398.
- Yang, W. (2003) Damage repair DNA polymerases, *Curr. Opin. Struct. Biol.* 13, 23–30.
- Prakash, S., Johnson, R. E., and Prakash, L. (2005) Eukaryotic translesion synthesis DNA polymerases: Specificity of structure and function, *Annu. Rev. Biochem.* 74, 317–353.
- Boudsocq, F., Kokoska, R. J., Plosky, B. S., Vaisman, A., Ling, H., Kunkel, T. A., Yang, W., and Woodgate, R. (2004) Investigating the role of the little finger domain of Y-family DNA polymerases in low fidelity synthesis and translesion replication, *J. Biol. Chem.* 279, 32932–32940.
- Hogg, M., Wallace, S. S., and Doublé, S. (2005) Bumps in the road: How replicative DNA polymerases see DNA damage, *Curr. Opin. Struct. Biol.* 15, 86–93.
- Ling, H., Boudsocq, F., Woodgate, R., and Yang, W. (2001) Crystal structure of a Y-family DNA polymerase in action: A mechanism for error-prone and lesion-bypass replication, *Cell* 107, 91–102.
- Ling, H., Boudsocq, F., Plosky, B. S., Woodgate, R., and Yang, W. (2003) Replication of a cis-syn thymine dimer at atomic resolution, *Nature* 424, 1083–1087.
- Ling, H., Sayer, J. M., Plosky, B. S., Yagi, H., Boudsocq, F., Woodgate, R., Jerina, D. M., and Yang, W. (2004) Crystal structure of a benzo[a]pyrene diol epoxide adduct in a ternary complex with a DNA polymerase, *Proc. Natl. Acad. Sci. U.S.A.* 101, 2265–2269.
- Ling, H., Boudsocq, F., Woodgate, R., and Yang, W. (2004) Snapshots of replication through an abasic lesion: Structural basis for base substitutions and frameshifts, *Mol. Cell* 13, 751–762.
- Zang, H., Goodenough, A. K., Choi, J.-Y., Irimia, A., Loukachevitch, L. V., Kozekov, I. D., Angel, K. C., Rizzo, C. J., Egli, M., and Guengerich, F. P. (2005) DNA adduct bypass polymerization by *Sulfolobus solfataricus* DNA polymerase Dpo4. Analysis and crystal structures of multiple base-pair substitution and frameshift products with the adduct 1,*N*<sup>2</sup>-ethenoguanine, *J. Biol. Chem.* 280, 29750–29764.
- Johnson, R. E., Prakash, L., and Prakash, S. (2005) Distinct mechanisms of cis-syn thymine dimer bypass by Dpo4 and DNA polymerase  $\eta$ , *Proc. Natl. Acad. Sci. U.S.A.* 102, 12359–12364.
- Nair, D. T., Johnson, R. E., Prakash, S., Prakash, L., and Aggarwal, A. K. (2004) Replication by human DNA polymerase- $\iota$  occurs by Hoogsteen base-pairing, *Nature* 430, 377–380.
- Johnson, R. E., Prakash, L., and Prakash, S. (2005) Biochemical evidence for the requirement of Hoogsteen base pairing for replication by human DNA polymerase  $\iota$ , *Proc. Natl. Acad. Sci. U.S.A.* 102, 10466–10471.
- Nair, D. T., Johnson, R. E., Prakash, L., Prakash, S., and Aggarwal, A. K. (2005) Rev1 employs a novel mechanism of DNA synthesis using a protein template, *Science* 309, 2219–2222.
- Haracska, L., Yu, S. L., Johnson, R. E., Prakash, L., and Prakash, S. (2000) Efficient and accurate replication in the presence of 7,8-dihydro-8-oxoguanine by DNA polymerase  $\eta$ , *Nat. Genet.* 25, 458–461.
- Carlson, K. D., and Washington, M. T. (2005) Mechanism of efficient and accurate nucleotide incorporation opposite 7,8-dihydro-8-oxoguanine by *Saccharomyces cerevisiae* DNA polymerase  $\eta$ , *Mol. Cell. Biol.* 25, 2169–2176.
- Zang, H., Irimia, A., Choi, J.-Y., Angel, K. C., Loukachevitch, L. V., Egli, M., and Guengerich, F. P. (2006) Efficient and high fidelity incorporation of dCTP opposite 7,8-dihydro-8-oxodeoxyguanosine by *Sulfolobus solfataricus* DNA polymerase Dpo4, *J. Biol. Chem.* 281, 2358–2372.
- Boudsocq, F., Iwai, S., Hanaoka, F., and Woodgate, R. (2001) *Sulfolobus solfataricus* P2 DNA polymerase IV (Dpo4): An archaeal DinB-like DNA polymerase with lesion-bypass properties akin to eukaryotic pol $\eta$ , *Nucleic Acids Res.* 29, 4607–4616.
- Vaisman, A., Hong, L., Woodgate, R., and Yang, W. (2005) Fidelity of Dpo4: Effect of metal ions, nucleotide selection and pyrophosphorolysis, *EMBO J.* 24, 1–11.
- Pelletier, H., Sawaya, M. R., Wolfle, W., Wilson, S. H., and Kraut, J. (1996) A structural basis for metal ion mutagenicity and nucleotide selectivity in human DNA polymerase  $\beta$ , *Biochemistry* 35, 12762–12777.
- Pelletier, H., and Sawaya, M. R. (1996) Characterization of the metal ion binding helix-hairpin-helix motifs in human DNA polymerase  $\beta$  by X-ray structural analysis, *Biochemistry* 35, 12778–12787.
- Pai, S.-C., Chen, T.-C., Wong, G. T. F., and Hung, C. C. (1990) Maleic acid/ammonium hydroxide buffer system for preconcentration of trace metals from seawater, *Anal. Chem.* 62, 774–777.
- Rech Koblit, O., Malinina, L., Cheng, Y., Kuryavyy, V., Broyde, S., Geacintov, N. E., and Patel, D. J. (2006) Stepwise translocation of Dpo4 polymerase during error-free bypass of an oxoG lesion, *PLoS Biol.* 4, 25–42.
- Kornberg, A., and Baker, T. A. (1992) *DNA Replication*, 2nd ed., Freeman, San Francisco.
- Castagnetto, J. M., Hennessy, S. W., Roberts, V. A., Getzoff, E. D., Tainer, J. A. and Pique, M. E. (2002) MDB: The metalloprotein database and browser at the Scripps Research Institute, *Nucleic Acids Res.* 30, 379–382.
- Cotton, F. A., Wilkinson, G., Murillo, C. A., and Bochmann, M. (1999) *Advanced Inorganic Chemistry*, 6th ed., John Wiley & Sons, New York.
- Minasov, G., Tereshko, V., and Egli, M. (1999) Atomic-resolution crystal structures of a B-DNA reveal specific influences of divalent metal ions on conformation and packing, *J. Mol. Biol.* 291, 83–99.
- Kragten, J. (1978) *Atlas of Metal–Ligand Equilibria in Aqueous Solution*, Halsted Press, Chichester, U.K.
- Westermann, K., Naser, K.-H., and Brandes, G. (1986) *Inorganic Chemistry*, 12th ed., pp 53–55, VEB Deutscher Verlag für Grundstoffindustrie, Leipzig, Germany.
- Hwang, H., and Taylor, J. S. (2005) Evidence for Watson–Crick and not Hoogsteen or wobble base pairing in the selection of nucleotides for insertion opposite pyrimidines and a thymine dimer by yeast DNA pol  $\eta$ , *Biochemistry* 44, 4850–4860.
- Bennett, R. M., Lehr, J. R., and McCarty, D. J. (1975) Factors affecting the solubility of calcium pyrophosphate dihydrate crystals, *J. Clin. Invest.* 58, 1571–1579.
- Xu, Y., Cruz, T. F., and Pritzker, K. P. (1991) Alkaline phosphatase dissolves calcium pyrophosphate dihydrate crystals, *J. Rheumatol.* 18, 606–610.